Aerosol Science and Technology, 43:425–441, 2009

ISSN: 0278-6826 print / 1521-7388 online
DOI: 10.1080/02786820802716735

Calibration of a Condensation Particle Counter Using a NIST Traceable Method

R. A. Fletcher, G. W. Mulholland, M. R. Winchester, R. L. King, and D. B. Klinedinst

National Institute of Standards and Technology, Gaithersburg, Maryland, USA

This work presents a calibration of a commercial condensation particle counter using National Institute of Standards and Technology (NIST) traceable methods. By the nature of the metrology involved, this work also compares the measurement results of three independent techniques for measuring aerosol concentration: continuous flow condensation particle counter (CPC); aerosol electrometer (AE); and the aerosol concentration derived from microscopic particle counting. Because of the transient nature of aerosol, there are no concentration artifact standards such as exist for particle diameter standards. We employ a mobility classifier to produce a nearly monodisperse, 80 nm, polystyrene latex aerosol. The test aerosol is used as a challenge for the CPC and the AE, and is subsequently filter sampled for electron microscopy. Our test stand design incorporates a continuous CPC aerosol concentration monitor to verify the aerosol stability. The CPC determines particle concentration by single particle counting at a constant sample flow rate. The AE has been calibrated to a NIST traceable current standard. The subsequent aerosol concentration measurement is obtained by determining the electrical current produced by a charged aerosol transported to the detector by a controlled aerosol flow rate. We have NIST traceability for flow rates for all methods and a methodology to calibrate the AE to NIST traceable electrical standards. The latter provides a calibration and a determination of the uncertainty in the aerosol derived current measurement. A bias in the measurements due to multiple charged particles was observed and overcome by using an electrospray aerosol generator to produce the challenge particles. This generator was able to produce aerosol concentrations over the range of 100 particles/cm^3 to 15 000 particles/cm^3 with lower number of dimer particles (≈1%). In our work, independent measurement of aerosol concentration is obtained by quantitatively collecting samples of the airborne polystyrene latex spheres on a small pore filter material and determining the number of particles collected by electron microscopy. Electron micrograph images obtained using a field-emission scanning electron microscope are analyzed using particle counting. We found the relative uncertainty in the aerosol electrometer measurements to be in excess of 100% for particle concentrations of approximately 120 particles/cm^3 and approximately 5% for concentrations above 6000 particles/cm^3. The uncertainty found by the microscopy method was approximately 3%.

Received 4 April 2008; accepted 31 December 2008.

Commercial equipment, instruments, and materials, or software are identified in this report to specify adequately the experimental procedure. Such identification does not imply recommendation or endorsement of these items by the NIST, nor does it imply that they are the best available for the purpose.

The authors gratefully acknowledge the contributions of the following NIST staff members David Buckingham, Jennifer Verkouteren, James Filliben, Jiann Yang, and Thomas Cleary. The authors would also like to acknowledge helpful discussions with S. Kaufman, F. Quant, B. Osmondson, and G. Sem all current or former TSI employees. This work was funded under the US Army/Calibration Coordination Group (CCG) and the NIST Office of Law Enforcement Standards (OLES).

Address correspondence to R. A. Fletcher, National Institute of Standards and Technology, 100 Bureau Drive STOP 8371, Gaithersburg, MD 20899, USA. E-mail: robert.fletcher@nist.gov

INTRODUCTION

Aerosol concentration measurements are important in a wide range of areas such as environmental studies, public health and hygiene work, manufacturing, clean room technologies, and quantitative fit testing for gas masks and protective garments. Although the focus of this work is to develop a traceable method for measuring aerosol concentration, the latter application is exceedingly important. Military personnel and first responders wear gas masks for protection against harmful agents such as combustion products, chemical vapors, and biological materials. The recognized potential global threat from chemical and biological agents demands that effective defensive measures be taken. An important part of this strategy is the testing and verification that assures secure gas mask fits via a quantitative fit test.

Quantitative gas mask fit tests measure and compare the ambient aerosol concentration outside of the fitted masks to the aerosol concentration inside. Small aerosol particles are used as a simulant for a harmful aerosol such as a viral agent as well as a surrogate gas test agent because they have nearly the same fluid dynamical properties as the airflow streams. The particles can be used to identify both leaks in the mask and inefficiencies in the filter. This technology is believed to provide a complete diagnostic of the integrity of the mask, the filter and the fit on the individual.

There are physical particle size standard reference materials and reference test materials such as NIST Standard Reference Materials for monodisperse polystyrene latex spheres and Arizona Road Dust that are designed to satisfy the need for particle size calibration. However, there are no aerosol concentration

standards (Liu 2004) and the research regarding aerosol concentration has not been as fully developed (Liu and Deshler 2003). The main reason for this deficiency is the time dependent losses of the aerosol particles. Thus an aerosol suspension cannot be transferred from one party to another as a calibration artifact such as a standard reference material for particle size.

Liu and Pui (1974) reported a method utilizing a charged aerosol, a differential mobility classifier and an aerosol electrometer (AE) to calibrate a condensation nuclei counter. Aerosol electrometer calibration has become a widely used approach to calibrate condensation particle counters (CPC) (Liu et al. 1975; Liu et al. 1982; Kesten et al. 1991; TSI 3022 manual). In our work, we expand on the AE calibration technique by calibrating the response of a commercial CPC widely used as a calibrant for both military and first responder quantitative fit test equipment with a NIST-traceable aerosol electrometer. This is, to our knowledge, the first time aerosol concentration measurements have been made traceable to NIST through an electrical current standard. Traceability is achieved in the measurement process by verifying the measurement properties or standards used in conjunction with the measurements against accepted national or international standards. A more definitive explanation can be found in the discussion section. Traceability for the aerosol electrometer required traceable low level current and air flow calibrants. Traceable measurements or standards become relevant to this calibration because we are attempting to calibrate an instrument (CPC) that has high precision with unknown accuracy by using a NIST traceable method that has lower precision, but quantifiable accuracy, i.e., some way to trace to the true aerosol concentration. Normally the calibrant has the highest precision, but in this case the calibrant has lower precision. The value of the AE is that it provides accuracy and NIST traceability. Since we do not have a standard aerosol generator that outputs known concentrations of aerosol, we are forced to compare the response of the CPC against other measurement technologies (AE and microscopy) that have been calibrated to traceable quantities.

In the past, a measurement bias was introduced due to multicharged particles. While the charging effect was accounted for by the theoretical charge distributions, it still contributed significantly to the measurement uncertainty (Liu et al. 1975). We eliminated this bias by electrospraying a suspension of monodisperse polystyrene latex spheres to produce singly charged test particles with almost no doubly charged particles.

Another difference in this study is in the concentration range of the aerosol. We have focused in the range from 1.0×10^2 particles/cm^3 to 2.0×10^4 particles/cm^3, which is the range of single particle counting for the CPC. The previous study by Liu et al. was for a concentration range of about 1.0×10^3 particles/cm^3 to 6.0×10^5 particles/cm^3. This range was convenient for testing the 1970 era CPCs which did not count individual particles.

We also used an independent method of determining the test aerosol concentration by means of quantitative particle collection by filtration followed by particle counting by electron microscopy and image analysis. The volume of aerosol flowing through the filter during the particle collection period is accurately determined.

EXPERIMENTAL DESIGN AND PROCEDURE

The calibration of a condensation particle counter with an aerosol electrometer was carried out using nominal 80 nm diameter solid polystyrene latex (PSL) spheres (Duke Scientific, Fremont, CA). Polystyrene latex spheres were incorporated into the experimental design to help reduce multiple charging of the aerosol and to enable microscopy. We followed the basic test stand design shown in Figure 1. The system consists of an aerosol generator (Collison aerosol generator), two diffusion dryers and an electrical charge neutralizer to produce primarily singly charged and neutral particles. The final test stand employed an electrospray aerosol generator and is described later in the article. The aerosol was "mobility band pass filtered" using a differential mobility analyzer (DMA) model 3080 made by TSI (Shoreview, MN) to produce a monodisperse 80 nm aerosol. To be mobility filtered the aerosol must be electrically charged. The flow rate of the monodisperse aerosol coming from the DMA was lower than the sum of the CPC and AE flow rates. Consequently, we sampled the monodisperse aerosol sequentially when doing the comparison of the CPC, AE, and microscopy. The particle size was chosen based on the fact that an 80 nm aerosol is used in several test facilities and that the CPC counts nearly 100% of the particles at this size. We employed a TSI model 3068 aerosol electrometer as an independent means of measuring the particle concentration. The AE measures the electrical current, I, that results from the flow of charged particles through this instrument. The relation between number concentration, N, of the aerosol and I is given by:

$$N = \frac{I}{Qe} \qquad [1]$$

where Q is the volumetric flow rate through the electrometer and e is the charge of an electron ($1.602\ 176\ 53(14) \times 10^{-19}$ C, (14) denotes uncertainty in these places) (Mohr and Taylor 2005).

Electrometer Calibration

The AE was calibrated before each use by a fA current source produced from a high precision voltage source and a nominal 100 GΩ resistor. Both the resistor properties and the voltage source were measured by the Electricity Division at NIST. The NIST voltage source had a relative uncertainty (u_V/V) of 5×10^{-6} and the resistor had a relative uncertainty (u_R/R) of $3.5 \times 10.^{-4}$ These measurements provide AE traceability to NIST through a current source traceable to the volt (Josephson junction) and a resistor traceable to the ohm (quantum Hall effect).

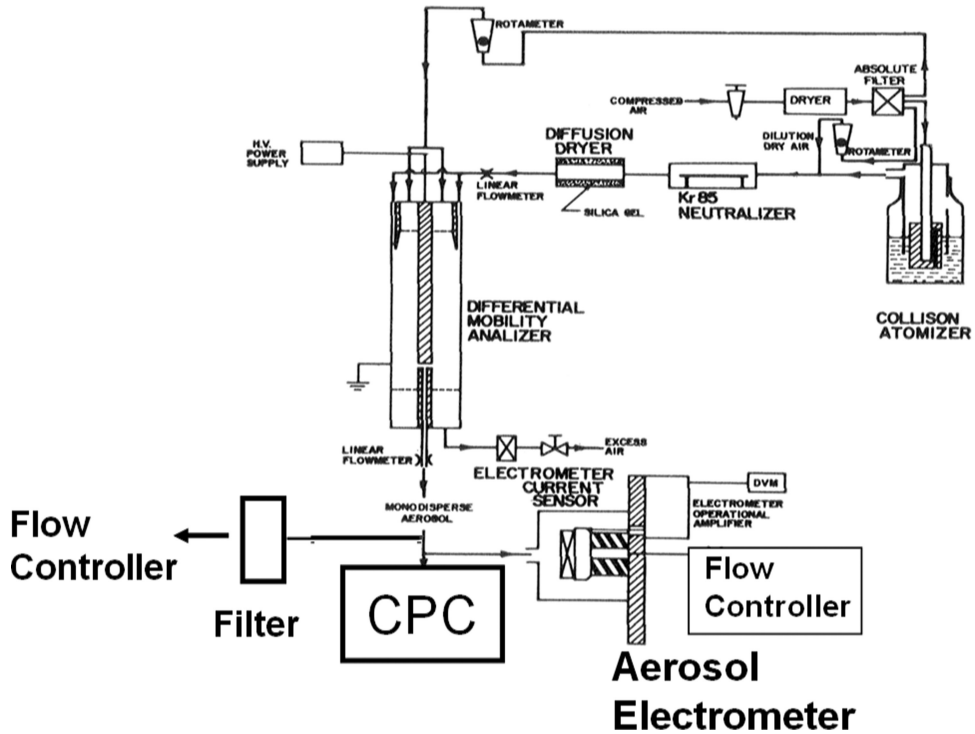

FIG. 1. Schematic of experimental apparatus that produces and conditions the aerosol for the CPC, AE, and filter tests. The instruments do not sample simultaneously, but in a sequential fashion (adapted with permission from Liu and Pui 1974).

Condensation Particle Counter

The condensation particle counter used in this study is a TSI model 3760A which operates only in the single particle count mode. No photometric transition occurs in this instrument. The flow rate is controlled by a critical orifice. The flow rates were determined for both the CPC and AE using a piston displacement meter (BIOS DryCal flow meter) that was calibrated with the NIST primary standard, the piston prover. The relative uncertainty was 0.0008 over the range of the measurements.

Filtration Method

As a second independent measurement, we determined the aerosol concentration by quantitative collection of the flowing aerosol onto a filter and counting the number of particles collected by scanning electron microscopy. The flow rate of the aerosol and the collection duration provide the aerosol volume collected. Filters used were polycarbonate with a 25 mm diameter and a 50 nm pore size. Since the pore size is approximately 60% less than the particle diameter, the 80 nm particles are captured with well over 99% efficiency (Green et al. 1991; He et al. 1987). The sample was gold-coated in a cold, Ar plasma and mounted in the Hitachi S-4500 field emission scanning electron microscope (SEM). The PSL spheres are difficult to differentiate from the carbon base filter substrate by SEM. However, the electron backscatter images of the Au coated spheres are clearly visible as shown in Figure 2a. The effective filtration area for particle collection is determined by collecting a large concentration of tungsten oxide particles on the filter. The diameter of the circular area covered by the tungsten particles is measured with a micrometer stage.

For the microscopic analysis, we randomly selected fields of view over the entire filter effective sample area including edge regions where the particle coverage decreases. Random sampling of the filter surface minimizes the effects of inhomogeneities in the particle coverage on the sample filter. For an SEM magnification of 20 000× we have a field-of-view area of approximately 32 μm^2. Images of approximately 25 to 250 fields for each sample were collected and stored for analysis. Automated image analysis was not used because image contrast often gave artifacts so each field was counted by visual inspection. All sample flow rates for the CPC, AE and filter were measured with low uncertainty using a BIOS DryCal flow meter that was calibrated by the Process Measurements Division at the NIST flow facility. The aerosol concentration is then determined by

$$N = \frac{N_m A_f}{V_a A_n} \qquad [2]$$

where N is the aerosol concentration, N_m is the number of particles counted in the SEM fields-of-view, A_f is the effective area of the filter, V_a is the volume of air sampled, and A_n is the area

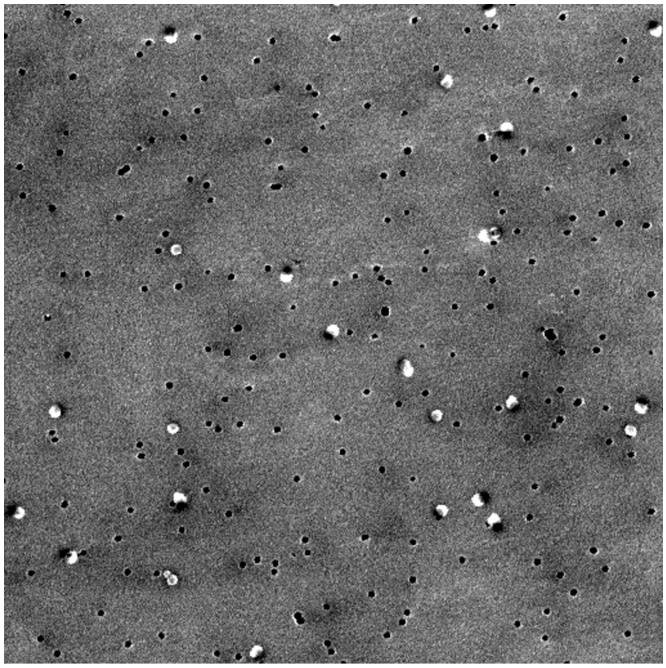

(a)

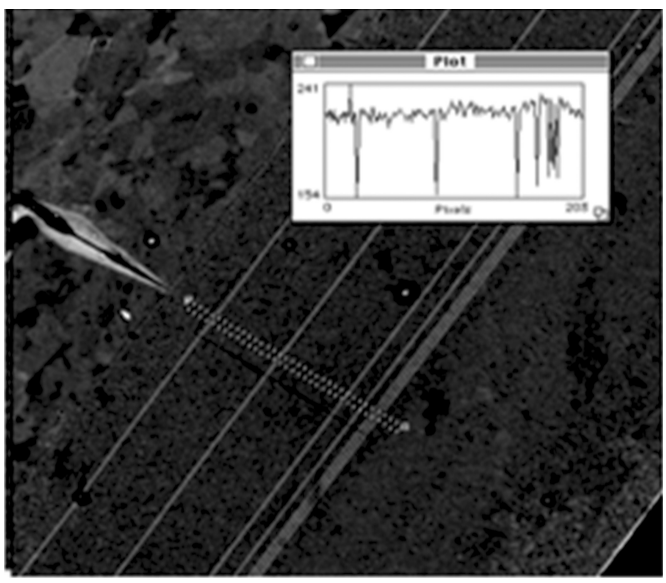

(b)

FIG. 2. (a) SEM backscatter image of polystyrene spheres on polycarbonate filter. The spheres appear as bright circular objects and the filter pores are the smaller dark areas. (b) is an electron micrograph of the SRM 484 g pitch standard used to spatially calibrate the images.

of the SEM fields-of-view. The quality A_n is dependent on the length determination in the square image. Our length measurements were made traceable to NIST through the application of SRM 484 g, a standard reference material SEM pitch standard. We calibrate the image space in both the horizontal and vertical directions. An example of a pitch measurement made on a SEM image is shown in Figure 2b.

The uncertainty in this microscopic determination of aerosol concentration is affected by all the variables on the right hand side of Equation (2). The uncertainty of each of these components as well as the combined uncertainty will be presented in the results section.

General Procedure for Calibration Measurements

The procedure for taking the CPC–AE calibration measurements is as follows. An electrode is installed into the AE replacing the aerosol filter, all electronics (including voltage source), CPC, DMA are turned on, cables are adjusted and the instrument allowed to stabilize for up to 24 h. Low fA current measurements require this precaution. Test currents over the range of 0 fA to 150 fA are applied through the electrode assembly to the AE and the response voltage from the electrometer is recorded. It is important to note that this set of measurements electronically calibrates the entire AE-data acquisition system from the electrometer to the computer interface. The electrode is removed and filter reassembled on the AE.

After this calibration is completed, then the aerosol generation system shown in Figure 1 is used to generate a 80 nm monodisperse aerosol. The CPC and AE are sequentially challenged with the aerosol being produced from the system. The concentration data from each instrument is computer recorded through independent interfaces. A blank measurement that results from passing clean air (void of aerosol) through the entire system including the DMA is recorded for each instrument and between each aerosol measurement. This blank is different from the voltage offset obtained in the electronic calibration. Five aerosol concentrations are produced and used to challenge both the AE and the CPC. In addition to the direct aerosol measurement, particles are collected for independent counting by microscopy. A filter housed in a sealed metal filter holder is used to quantitatively collect the aerosol for a known time period. Flow rates for all instruments and the filtration system are measured with the same traceable flow rate calibrant. Below we describe the experiments performed with the Collison nebulizer and with the electrospray generator, which was used in the most accurate measurements.

Collison Nebulizer Experiments

An eighty nanometer PSL aerosol is produced using the Collison nebulizer operating at approximately 207 kPa (30 psi). Five particle suspensions are used that provide aerosol concentrations ranging from approximately 120 particles/cm^3 to 13 000 particles/cm^3. For each day, the particle suspensions are randomly selected to avoid a systematic bias that might result from a sequential process. The DMA voltage is scanned to locate the singly charged monomer 80 nm particle population. An example of such a scan is shown in Figure 3.

The large peak is the singly charged monomer 80 nm particle. The small peak at approximately 1000 V is the doubly charged monomer and the broad peak at 3300 V is the singly

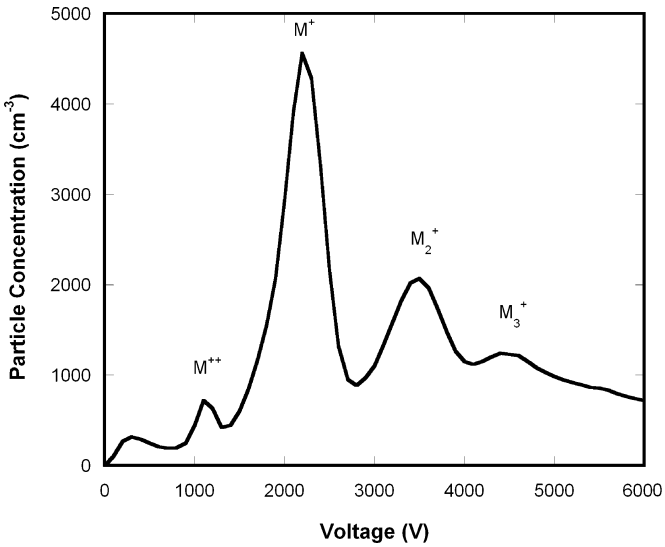

FIG. 3. DMA voltage scan of 80 nm polystyrene spheres nebulized from water suspension. M^{++}, M^{+}, M_2^{+}, and M_3^{+} are the doubly charged monomer peak, the singly charged monomer peak, the singly charged dimer peak, and singly charged trimer, respectively.

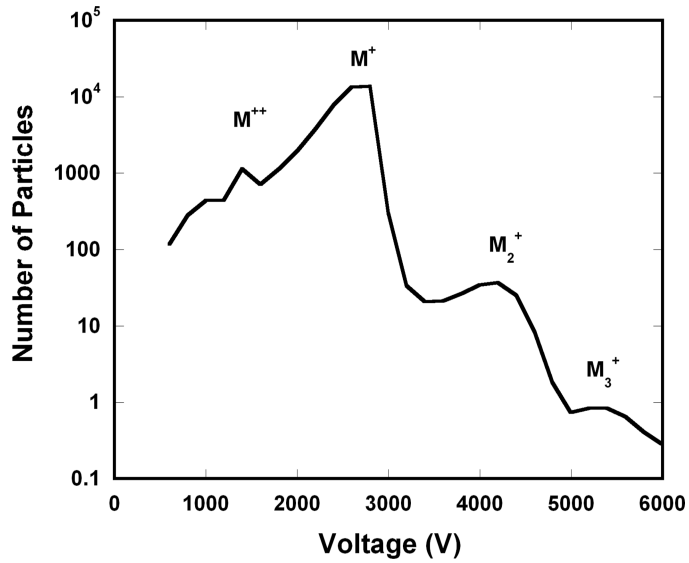

FIG. 5. DMA Voltage scan of aerosol produced by the electrospray aerosol generator. The plot shows monomer, dimer, and trimer populations on a semilog scale.

charged dimer. The DMA is then operated using the voltage (approximately 2 000 V) and flow rate associated with the peak of the 80 nm singly charged monomer particle.

Electrospray Aerosol Generator Experiments

An electrospray aerosol generator, TSI Model 3480, operating with a 40 μm diameter capillary was used to produce the PSL aerosol. Figure 4 shows a schematic of the electrospray generator along with the full measurement system. Suspensions were made of 1 drop to 3 drops of 80 nm PSL (nominal 1% solid spheres) per 1 mL of approximately 20 mmol/L ammonium acetate solution (conductivity of about 0.2 S/m). The electrospray method produces aerosol concentrations from 100 particles/cm^3 to approximately 17 000 particles/cm^3 with less than 1% single charged dimers. By comparison the Collison nebulizer had 20–30% single charged dimers. A typical voltage scan from the DMA is shown in Figure 5 illustrating the lack of clustered spheres. The log of the concentration is plotted to be able to show the very low concentration of doubly charged monomer, singly charged dimer and singly charged trimer particles relative to the singly charged monomer. In Figure 5, there is only 0.3% (37/13 800) singly charged dimers compared to singly charged monomers.

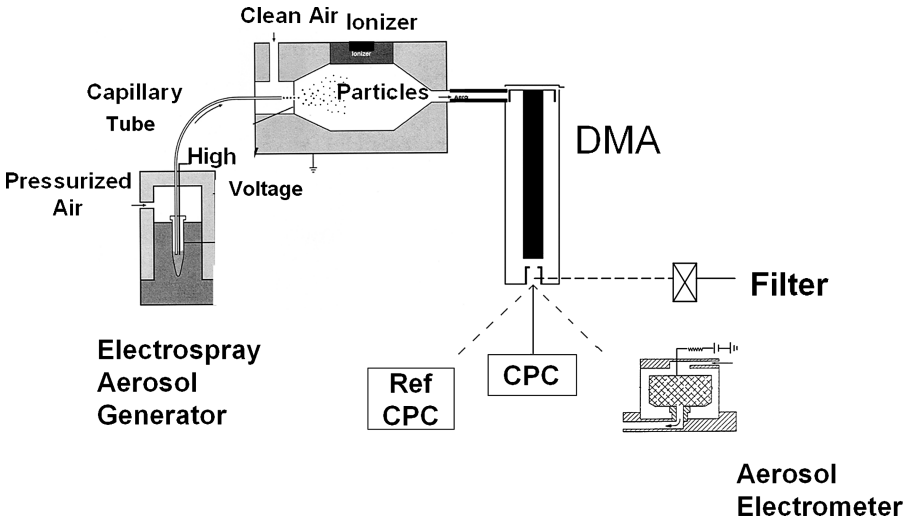

FIG. 4. Schematic of test stand used to compare the test CPC and AE. A low sample volume reference CPC was operated during the experiments and filters were collected for certain aerosol concentrations (adapted from TSI manual).

Experiments were designed to be conducted over 5 days. Each day an AE calibration was performed and 5 aerosol concentrations of the 80 nm PSL produced from the electrospray aerosol generator were used to compare the CPC and AE. For each day, two of the aerosol concentrations, 500 particles/cm^3 and 5 000 particles/cm^3 were always produced to measure day-to-day variability. The other 3 concentrations were chosen to be in the range of 100 particles/cm^3 to 12 000 particles/cm^3.

As shown in Figure 4, a second CPC, which operates at a low flow rate (300 mL/min), was used to sample the aerosol continuously over the experimental time frame. Data from this instrument were useful to compensate for drift in the output of the aerosol generator. Other differences from the configuration in Figure 1 are the placement of the neutralizer just downstream of the electrospray tip and the removal of the drier because of the much smaller drops and lower humidity. The DMA operated with flow rates of 20 L/min for sheath air and 2 L/min for monodisperse aerosol. The AE and the CPC sampled at 1.4 L/min and the filter collected the aerosol at 1 L/min. Each instrument was exposed to the test aerosol at a specified concentration for a duration of at least 300 s after the instrument readings stabilized. There were approximately 50 individual readings recorded during the test period.

RESULTS

Aerosol Electrometer Calibration

We calibrated the AE immediately before conducting each AE–CPC comparison experiment. The combined data are shown in Figure 6a for 5 data sets taken over several weeks. A linear least square regression of the data provides a relation between the voltage response of the electrometer and the applied current. The relation in terms for current, I, and Voltage, V, is

$$V = -3.02 \times 10^{-5} + 9.8163 \times 10^{11}\,(I) \qquad [3]$$

It is seen from Figure 6b that the distribution of the residuals (the difference between the measured value and the best fit line values) is independent of the applied current, a property that is relevant for the uncertainty analysis. The constancy of the residuals justifies the use of a linear regression model, which assumes that the error is independent of the size of the current.

The primary use of the V-I calibration curve is to relate the electrometer measurements to the current. In this case, one is interested in the value of I and its expanded uncertainty for a new value of the electrometer voltage V. Inverting Equation (3), one finds that:

$$I = \frac{V - b_0}{b_1} \qquad [4]$$

where b_0 is the V-intercept and b_1 is the slope of the line.

The expression for the uncertainty in a new value of I (Neter et al. 1990) is given by:

$$u\,(I) = \frac{\sigma_{res}}{b_1}\left[1 + \frac{1}{n} + \frac{\left(I - \bar{I}\right)^2}{\sum\left(I_i - \bar{I}\right)^2}\right] \qquad [5]$$

where σ_{res} is the standard deviation of the residuals, n refers to 33 data points in the calibration study, $\bar{I}$ to the average of the 33 values of I_i. The 95% confidence limit in I is given by:

$$I \pm t\,(1 - \alpha/2; n)\,u\,(I) \qquad [6]$$

where t is the Student t distribution and α equals 0.05. The uncertainty in I from the inverse prediction model for the regression at the 67% confidence interval is used in the calculation of the total uncertainty in the AE, which has a nominal value of 5.4×10^{-16} A.

AE–CPC Results for Collison Nebulizer (Preliminary Data Set)

A response comparison of the CPC and AE are shown in Figure 7 for the Collison nebulizer test facility. The CPC concentration values have been corrected using the measured flow rate of 1.41 L/min found for the electrospray measurements. These results reflect many measurement sessions over different days where each day the AE was calibrated using the method described above before the AE–CPC measurements were made. Each point corresponds to the mean of 10 measured concentrations by the CPC with a relative standard deviation in the range of 0.4%. The aerosol current was derived from the measured AE response voltage and the application of the AE current-voltage calibration. The blank (or background voltage) for the AE calibration was the empirical voltage determined by passing only clean air through the test stand and the AE. There were small background voltages (mean 0.00195 V) determined when passing clean air through the test stand and the AE. The background voltage values are possibly affected by residual charged air molecules and are slightly different than the electrically determined offset (background) voltage from the circuit calibration procedure. The calibration curve (Equation [3]) is used to convert the voltage reading from the AE to current values and then to aerosol concentration through Equation (1). The aerosol concentrations are not exactly the same from day to day, but the same aerosol population produced during that measurement session challenges each instrument.

The CPC data includes the directly measured results and the coincidence corrected concentration. The following equation (Gebhart 2001) is used in computing the coincident corrected concentration, N, from the measured number concentration, N_m

$$\frac{N}{N_m} = \exp(NQt_c) \qquad [7]$$

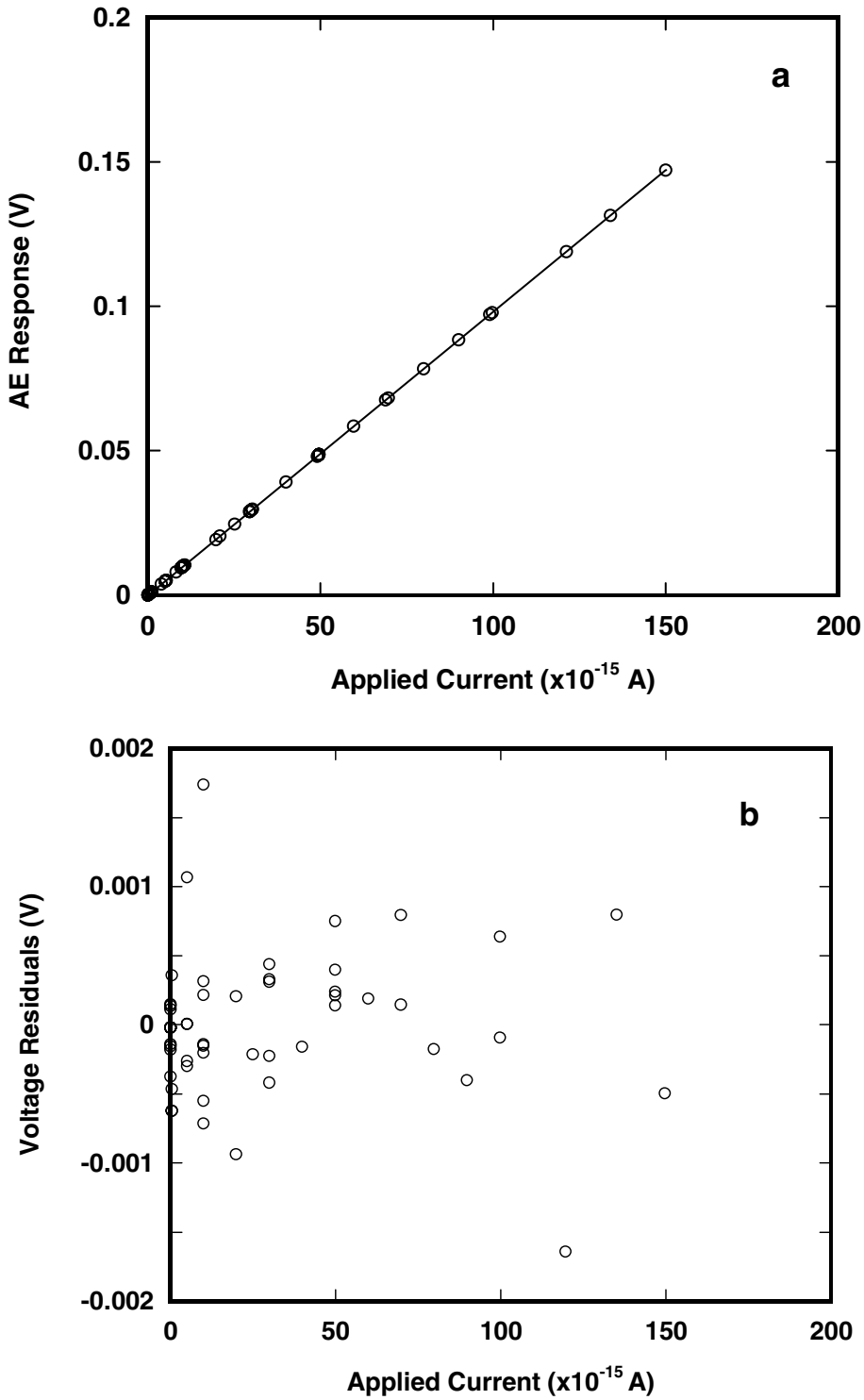

FIG. 6. Calibration curve of standardized applied current and AE voltage response (a) and the voltage residual plot (b).

where t_c, the measurement time is 0.4 μs (TSI manual) and the flow rate, Q, is determined in the experiments. It is seen that the coincidence corrected data agrees better with the ideal behavior of a 1:1 relation than the direct measurement, but the CPC value is still about 15% low relative to the AE. As we show below with the electrospray data, much of this difference can be accounted for by the presence of multiply charged multimers (dimers, trimers, etc.) from the Collison nebulizer. The other

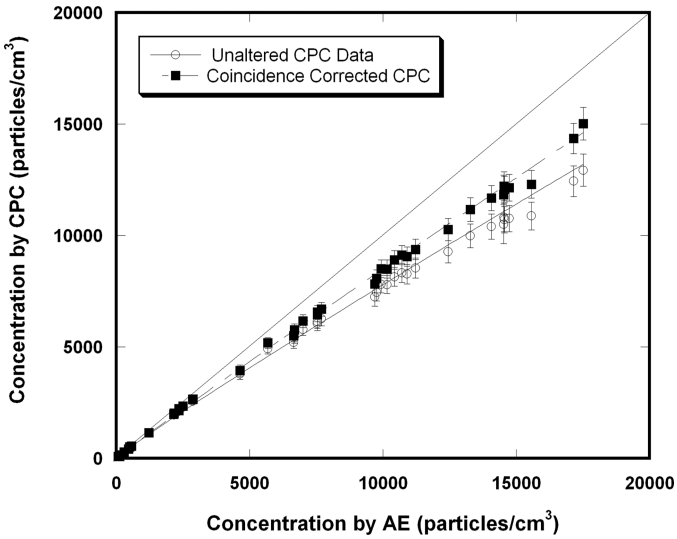

FIG. 7. Comparison of AE and CPC responses to the same 80 nm aerosol population produced by the Collison nebulizer. The unmodified data (open circles) and the coincidence counting correction to the CPC (solid squares). Line is a 1:1 relation for reference. The data are fitted with a power law expression similar in form to Equation (8).

issue with this measurement sequence is that the variation in the aerosol generator output is not monitored.

AE–CPC Results for Electrospray Aerosol Generator

Figure 8 shows a plot of the aerosol concentration data obtained for the AE and CPC measurements using the electrospray generator. Each point represents a mean value with at least 50 individual measurements. The CPC data have been normalized with the ratio of the mean concentrations of the continuous CPC

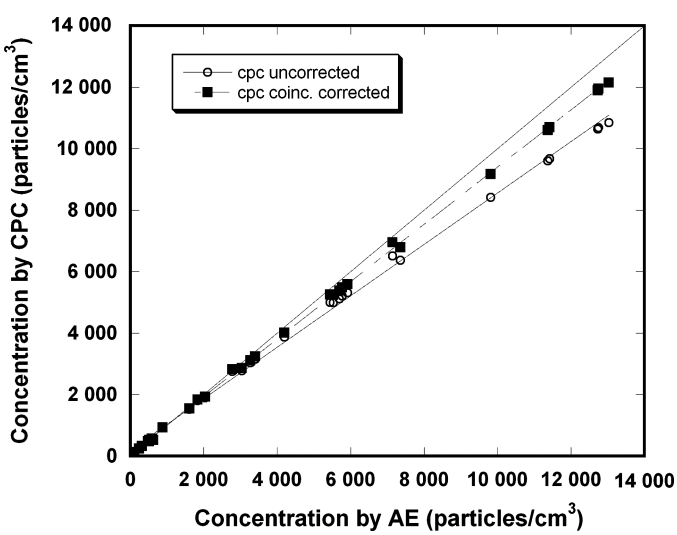

FIG. 8. Measured concentrations by CPC and AE plotted on a linear scale including uncorrected data (circles) and coincidence counting corrected points (squares). Aerosol was produced by the Electrospray Aerosol generator. Line is a 1:1 correspondence.

monitor for the periods of the AE data collection and the CPC data collection.

The linear least squares fit of the log of the concentration found by the CPC versus the log of the concentration found by the AE gives

$$\log_{10}(N_{CPC}) = 0.11658 + 0.95698 * \log_{10}(N_{AE}) \quad \text{or}$$
$$N_{CPC} = 1.308 N_{AE}^{(0.95698)} \qquad [8]$$

where N_{CPC} and N_{AE} are the aerosol concentration determined by the CPC and by the AE, respectively. The AE and CPC data were corrected to 298 K and 101.325 kPa. Equation (9) presents the expression for the regression line of CPC values that are coincidence, pressure, and temperature corrected.

$$\log(N_{CPC}) = 0.05213 + 0.98115 * \log(N_{AE}) \quad \text{or}$$
$$N_{CPC} = 1.127 N_{AE}^{(0.98115)} \qquad [9]$$

A log-log linear regression was preformed on the data rather than a simple linear regression for the reason given below. The mean and standard deviation of the CPC number concentration were obtained based on 33 sets of measurements each made over a period of 300 seconds. The following best fit relationship was obtained for the dependence of standard deviation for 33 values of N_{CPC}, σ_{CPC} , on N_{CPC}:

$$\sigma_{CPC} = 0.0355 N_{CPC}^{0.905} \qquad [10]$$

with a correlation coefficient of 0.958. In linear regression theory, the standard deviation of the y variable is assumed to be proportional or, at least, nearly proportional to the y variable for a $\log(y)$-$\log(x)$ linear regression and to be constant, independent of the y variable for a $y - x$ linear regression. In the case of the CPC number concentration, σ_{CPC} is nearly linear in N_{CPC} so that it is more appropriate to perform the regression using the logarithmic transform of the data. The use of a direct linear regression of the two number concentrations would provide biased estimators of the fit parameters because the standard deviation of the y variable is not even approximately a constant independent of the value of y.

The primary use of the calibration curve given by Equation (8) or Equation (9) will be in the calibration of a second CPC using the NIST traceable CPC. In this case, one is interested in the value of N_{AE} and its expanded uncertainty for a new value of the CPC number concentration, N_{CPC}. The most straightforward approach is to perform the analysis in terms of y and x where $y = \log(N_{CPC})$ and $x = \log(N_{AE})$. Inverting Equation (8) or Equation (9) one finds that:

$$x = \frac{y - b_0}{b_1} \qquad [11]$$

where b_0 is the y-intercept and b_1 is the slope of the line.

The expression for the uncertainty in a new value of x and the confidence interval are given by the same expressions as Equations (5) and (6) except that I is replaced with x and V with y. The confidence limits are expressed in terms of N_{AE} by using the relation between x and N_{AE} given above. The relative uncertainty in N_{AE} from the inverse prediction model for the regression at the 67% confidence interval, u_{reg}/N, is used in the calculation of the total uncertainty in the AE.

We note that the confidence interval obtained using the prediction model is approximately three times larger than the confidence limit for a point on the regression line. For the new value, there is an uncertainty in its location relative to the line in addition to the uncertainty associated with the linear fitting. The expression for the uncertainty for a point on the line is given by Equation (5) except the first term after the bracket (1) is missing.

Table 1 contains the AE-CPC comparison data and the total uncertainty ($\kappa = 1$; Taylor and Kuyatt, 1994) for the AE measurements. The quantitative uncertainty analysis is given in the next section. The concentrations by the CPC are presented for the coincidence uncorrected and corrected data.

Particle Concentration by Microscopy

For selected experiments, the aerosol concentration was also determined by scanning electron microscopy. Figure 9 provides an overview of the comparison between microscopy data and AE data. A line is drawn to indicate the 1:1 relationship between

TABLE 1
Data showing the comparison of the aerosol concentration determined by the AE, the CPC and the coincidence corrected CPC all three corrected to standard laboratory conditions, 298 K (25°C) and 101.325 kPa

Concentration by AE (particles/cm^3)	Uncertainty in AE Concentration (particles/cm^3)	Concentration by CPC No Correction (particles/cm^3)	Concentration by CPC Coincidence Corrected (particles/cm^3)
483.8	148.3	496.3	498.6
11 434.2	543.0	9 781.1	10 821.1
5 544.0	289.6	5 046.7	5 302.9
1 619.4	163.5	1 544.7	1 567.5
245.5	144.3	254.9	255.5
604.1	155.3	595.4	598.7
325.3	153.2	343.5	344.6
5 572.3	293.7	5 174.7	5 435.4
2 845.5	206.0	2 851.6	2 928.1
7 318.0	366.0	6 743.2	7 196.7
563.2	156.6	536.8	539.4
893.1	161.8	939.6	947.8
2 069.8	178.8	1 936.1	1 971.6
3 446.2	217.8	3 219.9	3 319.9
5 843.4	305.0	5 329.6	5 612.4
5 771.7	302.8	5 154.9	5 418.7
5 635.8	295.7	5 241.4	5 514.5
616.8	148.9	532.4	535.0
120.8	148.8	128.9	129.1
5 944.6	306.1	5 388.2	5 678.2
12 778.8	611.2	10 794.0	12 065.4
3 053.2	201.7	2 822.4	2 898.9
524.4	152.6	530.4	533.0
5 677.5	297.7	5 150.7	5 418.4
9 777.9	469.8	8 469.1	9 232.9
12 698.1	601.4	10 741.1	12 018.8
3 259.8	208.8	3 050.7	3 141.6
4 200.8	240.7	3 914.4	4 063.5
514.3	150.4	480.1	482.2
1 836.0	170.3	1 825.2	1 856.6
11 381.5	545.3	9 714.0	10 720.5
13 045.6	617.4	10 969.9	12 281.5
7 371.1	367.9	6 446.6	6 866.8

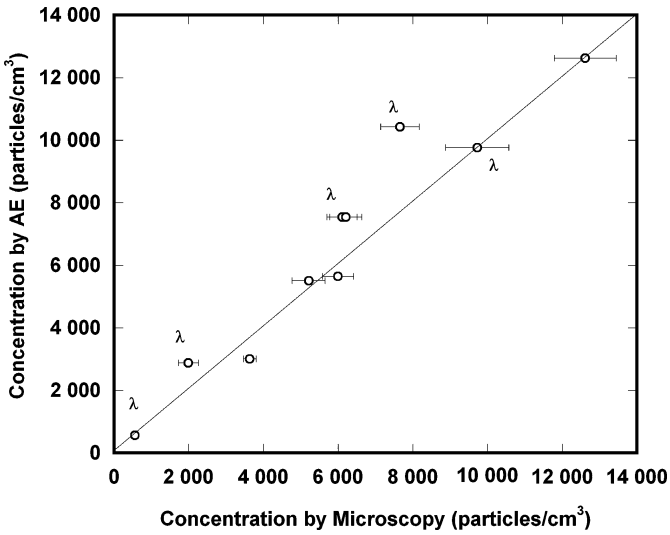

FIG. 9. Comparison of the aerosol concentration determined by microscopy and AE where λ denotes counts determined for agglomerated particles (Collison nebulized particles). The uncertainty bars correspond to the expanded uncertainty in the microscopy measurements. Double point at approximately 6000 particles/cm^3 corresponds to the concentration derived from two independent sets of images collected on the same filter. A 1:1 line is drawn for comparison.

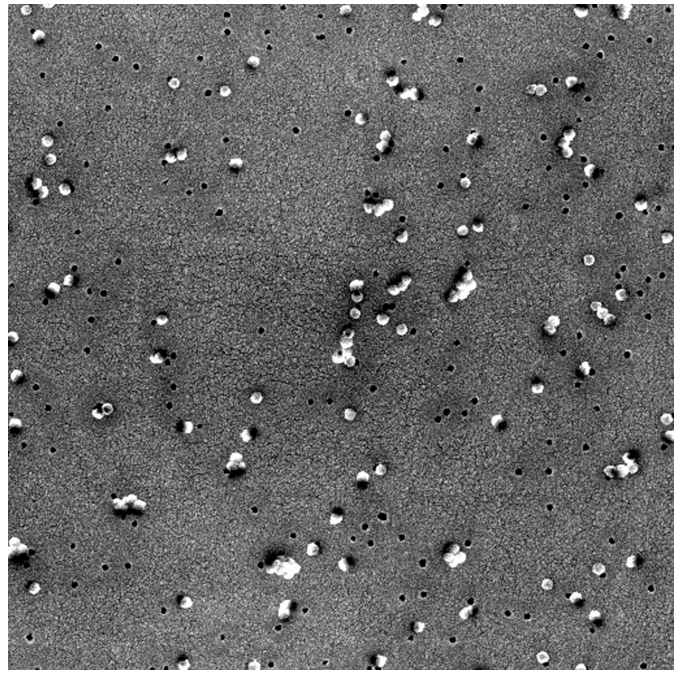

FIG. 10. SEM micrograph of 80 nm PSL monomers and multimers generated by the Collison nebulizer that have the same electrical mobility as the single 80 nm spheres.

the concentration determined by microscopy and by AE. It is seen that the results obtained using the Collison nebulizer, which are identified with λ in Figure 9, have a systematic discrepancy from the 1:1 line, while the results with the electrospray are closer to the 1:1 line. The exception, the data point obtained using the Collison nebulizer at a concentration near 10 000 particles/cm^3 lies very close to the line. This may be due to a drift in the aerosol generation by the Collison nebulizer. The aerosol concentration was measured only once by the AE during the 30 min to 60 min of aerosol generation by the Collison nebulizer, but it was measured continuously with the low flow CPC and a drift correction was made during the generation by the electrospray. A drift in the aerosol concentration produced by the Collison nebulizer may be responsible for the apparently good agreement between the AE measurement and the filter measurement for the one point at the concentration slightly less than 10 000 particles/cm^3.

Scanning electron microscopy was beneficial in uncovering a bias with the AE measurement. In Figure 10, it is evident that there are many agglomerated particles. Given the particle coverage density on the filter surface, it is unlikely that these agglomerates formed on the filter surface, rather they existed in the aerosol. To pass the 80 nm electrical mobility discriminator (the DMA) these agglomerates had to be multiply charged. From the mobility of the M_3^+ in Figure 3, we calculate the expected collection voltage of M_3^{++} to be 4 400 V/2 = 2 200 V which overlays the monomer peak. The doubly charged dimer M_2^{++} has a collection voltage of approximately 1 800 V with a broad peak. It is likely that the right side of the peak will contribute to the shoulder of the monomer 80 nm peak.

Agglomerated particles are most likely being produced from the Collison nebulizer for the higher concentration PSL sphere suspensions. In this system, the relatively large diameter droplets increase the probability that more than one PSL sphere resides in some of the drops and consequently upon drying forms a PSL cluster (Liu 2005). It is evident from Figure 3 that there is a relatively large percentage of singly charged dimer and trimer PSL particles. Some fraction of these dimers and trimers will have two charges with a mobility close to that of a singly charged monomer. So, the multi-charged clusters will not be effectively discriminated from the admitted test aerosol.

Table 2 provides a summary of the observed fraction of agglomerates for a range of concentrations. It is seen that the electrospray results are in the range of 1–2% while the Collison results are typically in the range of 8–9%.

UNCERTAINTY ANALYSIS

AE Uncertainty

An expression for the combined uncertainty in the AE measurement can be obtained from Equation (1) using the law of uncertainty propagation: (Taylor and Kuyatt 1994, p. 8).

$$\frac{u_N}{N} = \frac{\left[\left(\frac{\partial N}{\partial I}u_I\right)^2 + \left(\frac{\partial N}{\partial Q}u_Q\right)^2 + \left(\frac{\partial N}{\partial e}u_e\right)^2\right]^{1/2}}{N} \qquad [12]$$

TABLE 2
Number of agglomerates found by microscopy relative to the monomers observed

Nominal Concentration (particles/cm^3)	Number of Monomers Counted	Number of Agglomerates Counted	Fraction of Agglomeration
(Collison)			
500	1 032	90	0.080
2 000	1 055	105	0.090
6 000	1 653	147	0.082
8 000	1 654	506	0.234
10 000	988	95	0.088
(Electrospray)			
3 000	3 779	87	0.022
5 000	1 963	22	0.011
14 000	3 409	53	0.015

The partial derivative in Equation (12) can be expressed in terms of the relative uncertainties of the current, the flow rate and the charge of an electron.

$$\frac{u_N}{N} = \left[\left(\frac{u_I}{I}\right)^2 + \left(\frac{u_Q}{Q}\right)^2 + \left(\frac{u_e}{e}\right)^2\right]^{1/2} \qquad [13]$$

The relative uncertainty of the electronic charge is 8.5×10^{-8} and can be ignored. The uncertainty of the current and flow rate are made up of multiple components. A detailed listing of the components of the relative uncertainty is shown in Table 3. The uncertainty from V-I calibration regression component (0.54×10^{-15} A) contributes at each concentration (for example, at 5 000 particles/cm^3, 0.54×10^{-15} A / 20.5×10^{-15} A = 0.026). The second component is the voltage variability, which is a random or Type A uncertainty, and includes both the AE measurement voltage variability and the background voltage variability for the V-I calibration. The overall voltage variability is obtained from the square root of the sum of the squares of the standard uncertainties in the means for the AE measurement voltage and the background voltage. The V-I calibration component and the voltage variability component are given in Table 3 for a range of nominal concentrations. The uncertainty in the measured flow rate includes 3 components. The first is the uncertainty obtained in the calibration of the transfer standard to the primary NIST standard (0.11%), the second is the uncertainty found by linear regression of the test meter data and the transfer standard flow meter (0.085%), and the third is the flow rate variability uncertainty in the mean (n = 50) for the test meter (Type A). As indicated in Table 3, only the last of these uncertainty components varies with the concentration. The resulting values of u_I/I and u_Q/Q are presented in Table 4 along with the value of u_N/N computed using Equation (12) and the relative uncertainty, u_{reg}/N, associated with the CPC-AE regression. The total relative uncertainty u_T/N is computed as the quadrature sum of the combined relative uncertainty and u_{reg}/N.

The combined uncertainty for all of the AE data are shown in Figure 11. The relative uncertainty is high at 120 particles/cm^3 (approximately 123%) for values at low current (low particle concentration) domains. At these concentrations the AE cannot measure the aerosol signal over the electronic background (also discussed in the limits of detection below).

The original measurements by Liu and Pui (1974) report about 2% uncertainty for the electrical current measurements and about 1% in the flow rate with additional uncertainty due to multiple charging for an overall estimated uncertainty of about 5% in the calibration of the condensation nuclei counters using the DMA and AE charge counting approach. It is important to note that their measurements were conducted on aerosol concentrations up to approximately 300 000 particles/cm^3, concentrations an order of magnitude larger than the ones presented in our work. For such high concentrations, the uncertainty in the electrometer measurement is reduced by about an order of magnitude.

One possible bias in this calibration is from particle deposition in the AE sampling inlet tube. The diffusion loss of the

TABLE 3
Examples of the relative uncertainties associated with the various components contributing to the total uncertainty in the aerosol concentration determined by the AE

	Uncertainty in Current u_I/I		Uncertainty in Flow Rate u_Q/Q		
Nominal Concentration (cm^{-3})	V-I Calibration	Voltage Variability	Flow Rate NIST	Flow Rate Test Meter	Flow Rate Variability
120	1.227	0.091	0.0011	0.00085	0.00017
500	0.270	0.018	0.0011	0.00085	0.00018
3 000	0.046	0.005	0.0011	0.00085	0.00016
5 000	0.026	0.003	0.0011	0.00085	0.00011
12 000	0.013	0.002	0.0011	0.00085	0.00001

TABLE 4
The combined standard relative uncertainties for the aerosol concentration determination by the AE

Nominal Concentration (cm^{-3})	Uncertainty in Current u_I/I	Uncertainty in Flow Rate u_Q/Q	Combined Uncertainty u_N/N	Uncertainty CPC-AE Regression u_{reg}/N	Total Uncertainty u_T/N
120	1.230	0.0014	1.230	0.048	1.231
500	0.271	0.0014	0.271	0.046	0.274
3 000	0.046	0.0014	0.046	0.045	0.065
5 000	0.026	0.0014	0.026	0.045	0.052
12 000	0.013	0.0014	0.013	0.046	0.048

particles has been estimated as they flow through a 4.0 mm ID copper tube (1/4″ OD) 22 cm from the inlet to the Faraday Cage. Using the expression for diffusive losses in a laminar pipe flow (Friedlander 2000), the diffusion losses are found to be 0.2%. This bias is small compared to the measurement uncertainty and the measurements by the aerosol electrometer have not been corrected for this negligible bias.

Microscopy Counting Uncertainty

The uncertainty in the number concentration can be expressed in terms of the various terms of Equation (2) via the following equation:

$$\frac{u_N}{N} = \left[\left(\frac{u_{Nm}}{N_m}\right)^2 + \left(\frac{u_{Af}}{A_f}\right)^2 + \left(\frac{u_{Va}}{V_a}\right)^2 + \left(\frac{u_{An}}{A_n}\right)^2\right]^{1/2}. \quad [14]$$

To assure accurate area determination for each field-of-view, we found the variation of image area as a function of SEM stage height. We used the SRM 484 g SEM pitch standard to calibrate the stage viewed area at each height and between each filter measurement. Using SRM 484 g as the length standard (shown in Figure 4b) and varying the SEM stage height from 5 mm to 30 mm, we found that the length change was approximately 2 nm/mm of height. We make all of our measurements at a constant stage height of 15 mm. Even for a height variation of 1 mm, there would be minimal contribution of only ~4 nm^2 to the area compared to the entire field-of-view area that is approximately 3.2×10^7 nm.^{2} This effect is negligible compared to the other uncertainty components. The field-of-view calculation includes the uncertainty, as relative standard deviation, in the SRM 484 g SEM pitch standard (0.74%), and the uncertainty in the actual length measurements made on the SEM stage in both the vertical and horizontal directions. The nominal uncertainty was ≈0.60%, but varied with each measurement. The uncertainty in the effective filter area, $u_{Af} = 0.0168$ cm^2 for an area of 4.0811 cm^2 (A_f), was determined by repeated micrometer measurements of the effective circular filter diameter (as discussed in filter section above).

Table 5 presents a summary of the microscopy uncertainty. This table contains the mean number of particles per field-of-view (FOV), air volume sampled, and field-of-view area, the respective uncertainties and the total standard uncertainty. The uncertainty in mean number, u_{Nm}, contains the Type A

TABLE 5
Values and uncertainties (u_i) obtained for the particle concentration determination by microscopy. Listed are the mean values of the number of particles per field-of-view (FOV), the air volume sampled and the area of the field-of-view sampled. The uncertainty in the effective particle-covered filter area is 0.0168 cm^2 for an area of 4.0811 cm^2

N_m	u_{Nm}	V_a (cm^3)	u_{Va} (cm^3)	A_n (μm^2)	u_{An} (μm^2)	N (cm^{-3})	u_N (cm^{-3})
12.47	0.52	269 050	359	33.8	0.36	559.8	24.5
46.40	3.07	280 800	218	33.9	0.36	1 986.3	133
72.00	2.27	120 500	241	31.9	0.33	7 653	260.9
14.40	0.58	18 324	170	33	0.35	9 724.1	420.6
18.11	0.56	35 304	172	34.3	0.36	6 104.8	202.2
17.48	0.56	35 304	172	32.6	0.34	6 205.9	213.6
8.18	0.32	18 786	159	34.1	0.34	5 208.2	219.75
13.64	0.41	12 922	109	34.1	0.34	12 616.1	415.65
18.26	0.34	60 084	510	34.1	0.34	3 632.6	83.9
7.55	0.24	15 060	128	34.1	0.34	5 993.6	206.3

TABLE 6
Aerosol concentration determined for the same aerosol populations and the associated combined expanded uncertainty ($\kappa = 2$). The electrospray values have been temperature and pressure corrected. The CPC determined concentrations are coincidence corrected. The AE uncertainty includes the following components: voltage-current regression, the voltage variability, the flow rate, and the traceable voltage source and resistor. The AE expanded uncertainty does not contain the component due to the AE-CPC regression analysis

Concentration by Microscopy (particles/cm^3)	Expanded Uncertainty (particles/cm^3)	Concentration by AE (particles/cm^3)	Expanded Uncertainty (particles/cm^3)	Concentration by CPC (particles/cm^3)	Aerosol Generator
560	49	577		583	Collison
1 987	266	2 881		2 835	Collison
6 105*	404	7 545		6 858	Collison
6 206*	427	7 545		6 858	Collison
7 653	512	10 428		9 475	Collison
9 724	841	9 767		8 592	Collison
3 690	168	3 053	297	2 899	Electrospray
5 290	440	5 772	311	5 419	Electrospray
6 088	413	5 636	304	5 514	Electrospray
12 815	831	12 698	307	12 019	Electrospray

uncertainty due to non uniformity of the particle coverage on the filter surface since the fields of view are selected at random over the filter surface.

We have 10 independent measurements of particle concentration by microscopy on 9 filters that span the concentration range of interest and compare with the associated concentration measurements made by CPC and AE. Table 6 presents the aerosol concentrations measured by microscopy, CPC and AE, and their associated uncertainties over the range of approximately 500 particles/cm^3 to nearly 10 000 particles /cm^3. Since there is not sufficient data for a regression analysis for the microscopy data, the AE-CPC regression analysis uncertainty is not included in the calculation of the expanded uncertainty. This allows the two uncertainties to be compared on the same basis. The two microscopy measurements denoted by (*) found in Table 6 are independent values derived from the same filter, i.e., repeat count determinations from a new set of random fields-of-view.

A plot of these values presented in Figure 12 better illustrates the data. Note that the AE concentration almost always exceeds the CPC value. The spread in the electrospray data is much narrower in part due to the elimination of the multiple charge bias and to some extent, better stability in aerosol generation by the electrospray and the ability to correct any aerosol concentration drifts using the continuous CPC monitor (model 3022) that ran throughout the experiments (simultaneously for AE and test CPC 3760A). It is noted for the Collison Nebulizer data (Figure 12) that the CPC values exceed the microscopy values for four out of the six groups of concentration determinations. As discussed above, drift in the output of the Collison nebulizer may account for the lower microscopy determinations.

DISCUSSION

Coincidence Effect on the CPC Counting

It is apparent that the CPC undercounts with regard to the AE. There are several explanations for this difference. One, the CPC exhibits coincidence counting, where multiple particles are counted as one particle and this becomes increasingly important as the aerosol concentration increases. Coincidence counting error can be as large as 11% at concentration of 10 000 particles/cm^3. But at the same time, the AE current becomes more robust as the charged particle concentration (i.e., charge carriers) increases.

In optical particle counting it is possible to have two particles in the sensing volume at the same time, especially at high particle concentrations. In this case, the light scattering signal will be interpreted as one particle with an amplitude larger than the individual particles. This reduction in particle counts is referred to as the coincidence effect.

In discussing the coincidence effect, it is helpful to think in terms of the time dependent scattering signal of a particle as it enters the light beam. Once the light scattered from a single particle exceeds a threshold value, its time history will be tracked. The light scattering signal will increase as it traverses the more intense region of the Gaussian beam profile until it reaches a peak value. Near the time of peak intensity, the electrical signal is stretched to allow time for the signal to be read by the multichannel analyzer. During the recovery time of the electronics between successive count events, t_r, which includes the transit time (particle in the intense region of the light source) and the stretch time (pulse processing time of the multichannel analyzer), the presence of a new particle will not be counted as a second particle (Gebhart 2001).

As discussed by Gebhart (2001), there are various options in terms of the electronic configuration of the detector. The coincidence effect can be expressed as a ratio of the measured number concentration, N_m, to the number concentration, N. An approximate equation for describing the coincidence effect for less than a 10% loss in particle counts is given in terms of the volumetric flow rate Q and the counting time t_c by (Gebhart 2001):

$$\frac{N_m}{N} = \exp(-NQt_c) \quad \text{or} \quad \frac{N}{Nm} = \exp(NQt_c) \qquad [15]$$

The effective time that the particle is in the scattering volume for the CPC is about 0.4 μs (TSI manual) and Q is determined empirically in our experiments.

Even with the manufacturer's recommended coincidence correction for the CPC values, there is still a small deviation from perfect agreement between the two techniques. One explanation is that estimated parameters for the coincidence correction are average nominal values; there may be variations from instrument to instrument.

Multiple Charges

The AE bias is due to multiple charges on agglomerated particles. The microscopy shows the presence of agglomerated particles as illustrated in Table 2 and Figure 10. The experiment was designed to eliminate this charge effect (aerosol from a nebulized 80 nm PSL suspension instead of a solution), but the SEM images show the presence of a number of agglomerated particles. The DMA should filter dimer, trimer, and larger agglomerates from the transmitted aerosol because we are focusing the aerosol transmission through the singly charged, monomer 80 nm particle peak in the mobility scan. For an agglomerate to pass through the DMA, it must have nearly the same electrical mobility as the single particle. The only way for it to attain this mobility is by having multiple charges. Agglomerates and single 80 nm particles are counted each as individual particles in the CPC. Since the AE counts charges, this individual particle would not be counted as one particle as the CPC does, but as multiple particles. The bias in the CPC-AE, especially for the Collison nebulizer data most likely results from multiple charging of the PSL agglomerates.

Osmondson and Sem (2004) recommended the electrospray aerosol generator as a possible method to reduce clustering of the spheres. We believe that the electrospray generator has eliminated the multiple charged aerosol due to the small primary droplet size produced by this generator. The electrospray droplets are sufficiently small to contain only one or none of the 80 nm PSL particles. In fact about 1% was observed to have 2 particles.

Sensitivity of Electrometer

We calculated the limit of detection (L_d) and a critical limit (L_c) below which charge detection over background is not possible for the particular AE that we are using in these experiments (Currie 1968). Using the mean standard deviation of the background voltage, 0.000 262 2 V, we calculated the critical limit which is related to the background by

$$L_c = 1.64\,\sigma_b \qquad [16]$$

where σ_b is the standard deviation of the background. Using the same flow rates and the same AE calibration curve for the current used in our experiments, we obtained $L_c = 129$ particles/cm^3 and the limit of detection which is 3.29 times the background standard deviation to be 250 particles/cm.^{3} Liu and Pui (1974) reported that they had a noise level of approximately 125 particles/cm.^{3}

Estimates of Particle Loss in the CPC

Another explanation for the discrepancy between the calibration measurements is particle losses in the CPC. Particle loss was estimated by modeling the component processes in the CPC (Fletcher et al. 2007). The thermophoretic loss and diffusional loss in the condenser region were each estimated at 3% resulting in a total predicted loss of 6%. This value is slightly larger than the discrepancy of 4–5% observed between the electrometer measurement and the coincidence corrected CPC.

We point out that an estimate was also made for the losses in the nozzle at the exit of the condenser tube. Using a correlation obtained from a numerical flow dynamics study by Chen and Pui (1995), we estimated greater than 90% losses of the 10 μm droplets in the nozzle at the exit of the condenser tube. This is the droplet size expected from the alcohol condensation on the 80 nm spheres. This estimate is much greater than what has been observed in this calibration study. The cause of the discrepancy is not known.

The effects of particle charge and electric field variations have not been considered. The focus of the uncertainty analysis has been on the two calibration methods and not on the CPC, which is being calibrated by the other methods.

CPC Calibration

The primary focus of this study is to obtain a calibration curve and associated uncertainty for a CPC, which could then be used to make NIST traceable measurements or for calibrating other CPCs. Equations (8) and (9) express the CPC concentration as a function of the AE concentration. Since the aerosol electrometer is the calibration instrument, it is more appropriate to invert the equation to express the AE concentration (the true concentration) as a function of the CPC reading. The resulting expression is obtained for coincidence corrected and uncorrected, respectively:

$$N_{AE} = 0.885 N_{CPC}^{(1.019)} \qquad [17]$$

$$N_{AE} = 0.755 N_{CPC}^{(1.045)} \qquad [18]$$

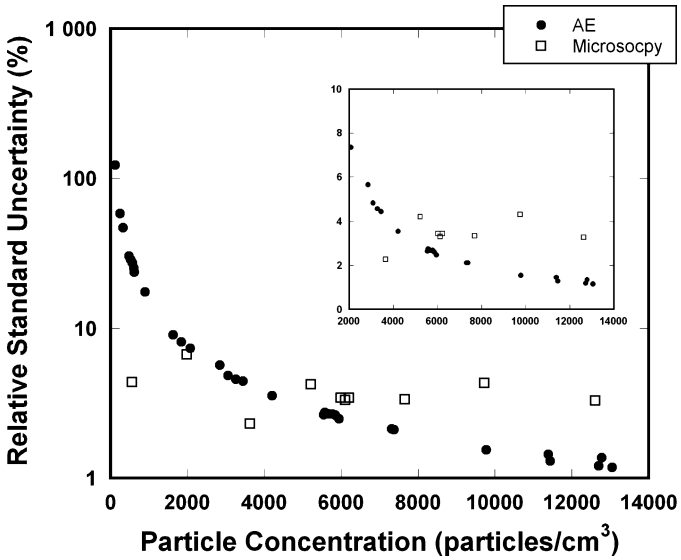

FIG. 11. The combined relative standard uncertainty, u_N/N (excluding the uncertainty component due to the regression) expressed as percent in the AE and microscopy measurements as a function of aerosol concentration.

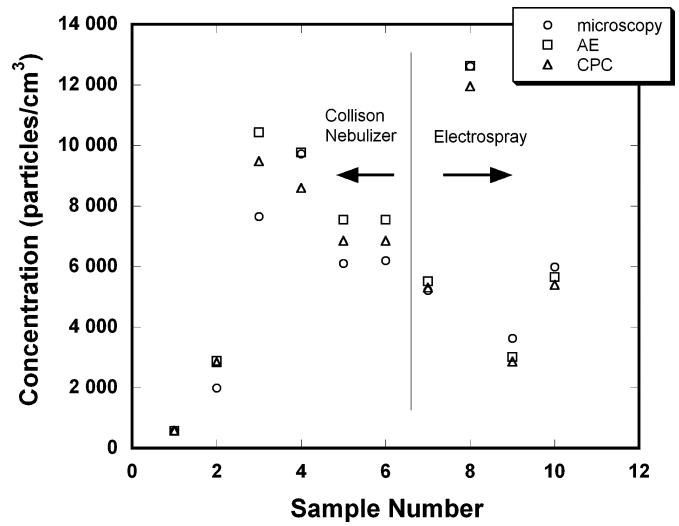

FIG. 12. Aerosol concentration measurement results comparing microscopy, AE and CPC for both the Collison nebulizer and the electrospray generated test aerosol.

The relative uncertainty (67%) for a range of concentrations is given in Tables 1 and 4 and it approaches a value of about 5% at concentrations greater than 5000 particles/cm^3. An essential component of the uncertainty analysis was making a proper estimate of the uncertainty associated with the regression fits for both the electrometer calibration and for the CPC-electrometer fit. The uncertainty of N_{AE} is estimated for a new value obtained with the CPC. If one computed the uncertainty in current based on a point on the $V - I$ calibration curve and then computed the uncertainty in N_{AE} based on a point on the calibration curve, one would underestimate the uncertainty by at least a factor of 3.

Electron Microscopy as an Independent Measurement Method

As seen in Figure 11, the estimated uncertainty in the number concentration for the aerosol electrometer measurements and the electron microscopy are similar for concentrations in the range of 3 000 particles/cm^3 to 5 000 particles/cm^3. Above 5 000 particles/cm^3, the electrometer has a slightly lower uncertainty, and below 3 000 particles/cm^3, the electron microcopy has a *significantly* lower uncertainty. This comparison is based on the uncertainty for the individual data points and does not include the regression analysis.

To attain the best possible aerosol filter collections, i.e., most representative and comparable to the AE and CPC, the aerosol concentration must be monitored throughout the collection period to account for drift in the aerosol generation. This was only done in the four measurements involving the electrospray. As shown in Figure 12, the filter and aerosol electrometer measurements agreed within 8% for three cases and differed by 20% in the fourth. These deviations do not indicate a large systematic bias. Thus microscopy provides an independent validation of the aerosol electrometer measurements. However, we also point out that the deviation between the two types of measurements is greater than expected given the measurement uncertainties.

There are not enough microcopy measurements to fully assess the uncertainty associated with the repeatability in the measurement process. For this reason there is no regression analysis for the microcopy and no predictions of the uncertainty in a predicted new measurement point for the microcopy.

While the microcopy is labor intensive, it has value in obtaining significantly lower uncertainty results for aerosol concentrations less than 3 000 particles/cm^3. If the particle counting could be automated, this could be a useful measurement method. Perhaps semiconductor wafer deposition and scanning technology could be applied to this metrology problem. In this case, the particles would be deposited electrostatically on a silicon wafer rather than via filtration and the counting would be done by light scattering from particles on the surface rather than via electron microscopy. This is routinely done in semiconductor fabrication for particles as small as 60 nm. The number of particles deposited on the wafer could be far fewer than for the filter because every particle would be counted.

Traceability

Many of the measurements in this work were made traceable to NIST primary standards or to the International System of Units (SI), the metric system agreed upon throughout the world. A widely accepted definition (Ehrlich and Rasberry 1998) for traceability found in the Vocabulary of Basic and General Terms in Metrology 1993 is "property of the result of a measurement or the value of a standard whereby it can be related to stated references, usually national or international standards, through an unbroken chain of comparisons all having stated uncertainties."

Traceability does not guarantee the measurement results are "true" or accurate, but rather there is a higher standard to reference the measurement (Larrabee and Postek 1993). Sometimes this standard may be a consensus standard where the value is accepted or agreed upon by a large number of users in a technical community. Accuracy, a highly desirable measurement goal, is achievable through calibration to an accurate higher standard with the understanding that the uncertainties in the standard and in the calibration and in the measurement process can be determined. Traceability to a widely accepted higher standard permits comparisons of measurements among users. It also provides a benchmark for reproducing experiments (or products) and serves to satisfy audits, legal issues, or provide a measure of goodness to a product (Ehrlich and Rasberry 1998). Traceability for the aerosol electrometer was through calibration to a low level current generated by a circuit in which the components are referenced to NIST standards that in turn are referenced to the volt (Josephson junction) and the ohm (quantum Hall effect). Our flow rates were made traceable to the NIST volumetric prover. The SEM field-of-view dimensions, critical to determining the aerosol concentration by microscopy, are traceable through the Standard Reference Material 484 g, an SEM pitch standard that is in turn traceable to the meter by optical interferometry.

SUMMARY AND CONCLUSIONS

In summary, we have developed a method to measure particle concentration based on NIST traceable electrical current measurements using a calibrated aerosol electrometer. Particle counting by microscopy is utilized as an independent first principle method of determining particle concentration. An electrospray aerosol generator was shown to produce 80 nm aerosol particles with virtually no dimers and thus no multiple charge, but with aerosol concentrations spanning the range of interest. We have been able to calibrate the specific CPC used in these experiments and derive a relationship between the corrected and uncorrected coincidence CPC response for aerosol concentration and a concentration obtained from a NIST traceable electrometer.

The calibration technique is sensitive enough to reveal a bias in the methods due to multiply charged particles. We think that there is a bias in the AE data collected using the Collison nebulizer and that it is due to particle agglomerate formation from droplet evaporation and multiple charging of these agglomerates. SEM micrographs bear this out and the fact that the divergence of the AE–CPC data is most pronounced for high particle concentration is further evidence. By using the electrospray aerosol generator, we were able to greatly reduce agglomeration and thus multiple charge effects that caused an approximate 6% bias in the measurement. As a consequence, the spread among the three independent methods of measuring aerosol concentration has been reduced.

An expression for the correct concentration (N_{AE}) as a function of the CPC concentration is obtained for using the CPC to make traceable measurements. The uncertainty is given for N_{AE} based on a new CPC measurement. We report a concentration dependent uncertainty in the AE measurements ranging from 27% for 500 particles/cm^3 to 6.5% for 3 000 particles/cm^3 to 4.8% at 12 000 particles/cm^3. This includes the uncertainty due to the CPC-AE regression analysis. Without the regression uncertainty, the corresponding concentrations had uncertainties of 27%, 4.6%, and 1.3%, respectively. The microscopy measurements that do not include the regression analysis uncertainty have approximately 3% uncertainty for all concentrations. The uncertainties found for high concentration aerosol is comparable to the uncertainty reported by Liu and Pui (5%). Data is also presented showing a comparison among the three concentration measuring techniques for both Collison nebulizer and Electrospray generated aerosol. Model simulations of aerosol loss in the CPC (as a way of estimating the Type B uncertainty) indicate that there could be upwards of 6% loss due to all identified mechanisms. The experimental results indicate that there is less aerosol loss in the CPC tested.

REFERENCES

Ahn, K.-H., and Liu, B. Y. H. (1990). Particle Activation and Droplet Growth Processes in Condensation Nucleus Counter—I. Theoretical Background, *J. Aerosol Sci.* 21(2):249–261.

Ahn, K.-H., and Liu, B. Y. H. (1990). Particle Activation and Droplet Growth Processes in Condensation Nucleus Counter—II. Experimental Study, *J. Aerosol Sci*. 21(2):263–275.

Alofs, D. J., Lutrus, C. K., Hagen, D. E., Sem, G. J., and Blesener, J. L. (1995). Intercomparison Between Commerical Condenstaion Nucleus Counters and an Alternating Temperature Gradient Cloud Chamber, *Aerosol Sci. Technol*. 23:238–249.

Biermann, A., and Nergman, W. (1984). Measurement of Aerosol Concentration as a Function of Size and Charge, *Aerosol Sci. Technol*. 3:293–304.

Chen, D.-R., and Pui, D. Y. H. (1995). Numerical and Experimental Studies of Particle Deposition in a Tube with a Conical Contraction-Laminar Flow Regime. *J. Aerosol Sci.* 26:563–574.

Currie, L. A. (1968). Limits of Quantitative Detection and Quantitaive Determination: Applications to Radiochemistry, *Anal. Chem.* 40:586–593.

Ehrlich, C. D., and Rasberry, S. D. (1998). Metrological Timelines in Traceability, *J. Res. Nat. Inst. Stand. and Technol.* 103:93.

Fletcher, R., Mulholland, G., Yang, J., King, L., Winchester, M. Klinedinst, D., Verkouteren, J., Buckingham, D., Cleary, T., and Filliben, J. (2007). Verification of a Gas Mask Calbrant, *National Institute of Standards and Technology Internal Report* NIST IR 7424.

Friedlander, S. K. (2000). *Smoke, Dust, and Haze: Fundamentals of Aerosol Dynamics.* (2nd edition), Oxford University Press, New York.

Gebhart, J. (2001). Optical Direct-Reading Techniques: Light Intensity Systems, in *Aerosol Measurements: Principles, Techniques, and Applications,* P. A Baron and K. Willeke, ed., Wiley-InterScience, Inc.

Green, B., Ratnikov, B., Stofer, D., and Aicholtz, P. (1991). How the Latex Sphere Challenge Impacts on Submicron Membrane Ratings. Presented at the annual meeting of the American Filtration Society (1991).

He, L., Alling, D., Popkin, T., Shapiro, M., Alter, H., and Purcell, R. (1987). Determining the Size of Non-A, Non-B Hepatitis Virus by Filtration, *J. Infect. Dis*. 156 No. 4:636.

International Vocabulary of Basic and General Terms in Metrology. (1993). 2nd edition, BIPM, IEC, IFCC, ISO, IUPAC, IUPAP and OIML, International Organization for Standardization, Geneva.

Kesten, J., Reineking, A., and Portendorfer, J. (1991). Calibration of a TSI 3025 Ultrafine Condensation Particle Counter, *Aerosol Sci. Technol*. 15:107–111.

Larrabee, R. D., and Postek, M. T. (1993). Precision, Accuracy, Uncertainty and Traceability and Their Application to Submicrometer Dimensional Metrology, *Solid-State Electron.* 36(5):673–843.

Liu, P. S. K., and Deshler, T. (2003). Causes of Concentration Differences Between a Scanning Mobility Particle Sizer and a Condensation Particle Counter, *Aerosol Sci. Technol*. 37:916–923.

Liu, B. Y. H., and Pui, D. Y. H. (1974). A Submicron Aerosol Standard and Primary, Absolute Calibration of the Condensation Nuclei Counter, *J. Coll. Interf. Sci.* 47 No. 1:156–171.

Liu, B. Y. H., Pui, D. Y. H., Hogan, A. W., and Rich, T. A. (1975). Calibration of the Pollak Counter with Monodisperse Aerosols, *J. Appl. Meteorol.* 14 (1):46–51.

Liu, B. Y. H., Pui, D. Y. H., McKenzie, R. L., Agarwal, J. K., Jaenicke, R., Pohl, F. G., Preining, O., Reischl, G., Szymanski, W., and Wager, P. E. (1982). Intercomparison of Different "Absolute" Instruments for Measurement of Aerosol Number Concentration, *J. Aerosol. Sci.* 13(5):429–450.

Liu, B. Y. H. (2004). Presentation. American Association for Aerosol Research Annual Conference.

Liu, B. Y. H. (2005). Private Communication.

Mohr, P. J., and Taylor, B. N. (2005). *Rev. Mod. Phys*. 77:1. Also CODATA Recommended Values of the Fundamental Physical Constants: 2002 NIST SP 961 (Dec. 2005).

Natrella, M. G. (1963). *Experimental Statistics*. National Bureau of Standards Handbook 91. U.S. Department of Commerce. U.S. Government Printing Office, Washington, D.C.

Neter, J., Wasserman, W., and Kutner, M. H. (1990) *Applied Linear Statistics Models, Regression, Analysis of Variance, and Experimental Design*. Irwin, Boston, MA, 3rd edition, p. 175.

Osmondson, B., and Sem, G. (2004). Private Communication.

Snedecor, G. W., and Cochran, W. G. (1989).*Statistical Methods.* Iowa State University Press, Ames, Iowa, 8th edition, p. 170–

Stolzenburg, M. R., and McMurry, P. H. (1991). An Ultrafine Aerosol Condensation Nucleus Counter, *Aerosol Sci. Technol*. 14:48–65.

Taylor, B. N., and Kuyatt, C. E. (1994). Guidelines for Evaluating and Expressing the Uncertainty of the NIST Measurement Results. NIST Technical Note 1297. U.S. Government Printing Office, Washington, DC.

TSI model 3760A Instrument Manual. TSI, Shoreview, MN.

Van der Meulen, Plomp, A., Oeseburg, F., Buringh, E., van Aalst, R. M., and Hoevers, W. (1980). Intercomparison of Optical Particle Counters Under Conditions of Normal Operation, *Atmos. Environ.* 14:495–499.

Zhang, Z., and Liu, B. Y. H. (1991). Performance of TSI 3760 Condensation Nuclei Counter at Reduced Pressures and Flow Rates. *Aerosol Sci. Technol*. 15:228–238.

Zhang, Z., and Liu, B. Y. H. (1990). Dependence of the TSI 3020 Condensation Nucleus Counter on Pressure, Flow Rates and Temperature, *Aerosol Sci. Technol*. 13:493–504.